

# 3D multimodal image fusion based on MRI in the preoperative evaluation of microvascular decompression: A meta-analysis

CHEN LIANG<sup>1,2</sup>, LING YANG<sup>3</sup>, BINBIN ZHANG<sup>1</sup>, RUICHUN LI<sup>1</sup> and SHIWEN GUO<sup>1</sup>

<sup>1</sup>Department of Neurosurgery, The First Affiliated Hospital of Xi'an Jiaotong University, Xi'an, Shaanxi 710061, P.R. China; <sup>2</sup>Department of Diagnostic and Interventional Radiology, Division of Medical Physics, University Medical Center Freiburg, Faculty of Medicine, University of Freiburg, D-79106 Freiburg im Breisgau, Germany; <sup>3</sup>Department of Aviation Psychology Research, Xi'an Civil Aviation Hospital, Xi'an, Shaanxi 710082, P.R. China

Received 28 September 2022; Accepted February 14, 2023

DOI: 10.3892/etm.2023.11870

**Abstract.** Neurovascular compression (NVC) is the main cause of hemifacial spasm (HFS) or trigeminal neuralgia (TN), and frequently occurs at the root entry zone of cranial nerves. Microvascular decompression (MVD) is an effective surgical treatment for TN and HFS caused by NVC. The accurate preoperative diagnosis of NVC is crucial to the evaluation of MVD as an appropriate treatment for TN and HFS. Three-dimensional (3D) time-of-flight magnetic resonance angiography (3D TOF MRA) and high resolution T2-weighted imaging (HR T2WI) are used to detect NVC prior to MVD; however, this combination alone has certain disadvantages. Multimodal image fusion (MIF) may combine two or more images from the same or different modalities, allowing neurosurgeons to use the reconstructed 3D model to observe anatomical details more clearly from different perspectives. The aim of the present meta-analysis was to evaluate the effect of 3D MIF based on 3D TOF MRA combined with HR T2WI in the preoperative diagnosis of NVC, and thus to evaluate its clinical application value in the preoperative evaluation of MVD. Relevant studies available on PubMed, Embase, Web of Science, Scopus, China National Knowledge Infrastructure and the Cochrane Library, and published from the inception of each database to September 2022, were retrieved. Studies using 3D MIF based on 3D TOF MRA combined with HR T2WI to diagnose NVC in patients with TN or HFS were included. The Quality Assessment of Diagnostic Accuracy Studies checklist was used to evaluate the quality of the included studies. The statistical software Stata 16.0 was used to perform the meta-analysis. Data extraction was performed by two

independent investigators and discrepancies were resolved by discussion. Pooled sensitivities, specificities, positive likelihood ratio (PLR), negative likelihood ratio (NLR), diagnostic odds ratio (DOR) and the area under the receiver operating characteristic curve (AUROC) were calculated as the main summary effect size. The  $I^2$  and Q-test were used to assess heterogeneity. The present search identified 702 articles, of which 7 (comprising 390 patients) fulfilled the inclusion criteria. Bivariate analysis indicated that the pooled sensitivity and specificity of 3D MIF based on 3D TOF MRA combined with HR T2WI for detecting NVC were 0.97 (95% CI, 0.95-0.99) and 0.89 (95% CI, 0.77-0.95), respectively. The pooled PLR was 8.8 (95% CI, 4.1-18.6), the pooled NLR was 0.03 (95% CI, 0.02-0.06) and the pooled DOR was 291 (95% CI, 99-853). The AUROC was 0.98 (95% CI, 0.97-0.99). The studies had no substantial heterogeneity ( $I^2=0$ ;  $Q=0.000$ ;  $P=0.50$ ). The present results suggested that 3D MIF based on 3D TOF MRA combined with HR T2WI had excellent sensitivity and specificity for diagnosing NVC in patients with TN or HFS. Therefore, this method should serve a key role in MVD preoperative evaluation.

## Introduction

Neurovascular compression (NVC) is the main cause of primary trigeminal neuralgia (TN) or hemifacial spasm (HFS), and frequently occurs at the root entry zone (REZ) of cranial nerves (1). Microvascular decompression (MVD) is an effective surgical treatment for TN and HFS caused by NVC (2,3). However, preoperative detection of NVC is occasionally difficult. Although MVD is not challenging for skilled and experienced neurosurgeons, it is not effective for patients with TN or HFS not caused by NVC (4). Therefore, an accurate preoperative diagnosis of NVC is crucial in deciding whether to perform MVD.

Magnetic resonance imaging (MRI) has been used to detect NVC prior to MVD for numerous years; however, it does have certain disadvantages. Routine MRI sequences cannot clearly and accurately display the relationship between nerves and blood vessels at the REZ (4). Since the 1990s, 3D time-of-flight magnetic resonance angiography (3D TOF MRA) has gradually become a common MRI sequence for detecting NVC. 3D TOF MRA is able to selectively image fast-flowing blood and clearly

---

*Correspondence to:* Professor Shiwen Guo, Department of Neurosurgery, The First Affiliated Hospital of Xi'an Jiaotong University, 277 Yanta West Road, Xi'an, Shaanxi 710061, P.R. China  
E-mail: guoshiwen1962@126.com

**Key words:** 3D multimodal image fusion, magnetic resonance imaging, 3D time-of-flight magnetic resonance angiography, high resolution T2-weighted imaging, neurovascular compression, microvascular decompression, meta-analysis

display nerves and blood vessels (5). However, the 3D TOF MRA sequence demonstrates a poor ability to visualize blood vessels with a slow blood flow, such as veins and arterioles (6). With the development of MRI technology, the appearance of high resolution T2-weighted imaging (HR T2WI) brings new options for NVC detection. HR T2WI may adequately demonstrate the anatomical structure in the cerebellopontine angle (CPA) against the background of cerebrospinal fluid (CSF) signal and aid in justifying a diagnosis of NVC, which may be obtained by different technologies, including 3D balanced steady state gradient echo and 3D fast turbo spin echo (5). Different manufacturers use different names for these technologies, such as constructive interference steady state (CISS), fast imaging employing steady-state acquisition (FIESTA), balanced fast field echo (bFFE), sampling perfection with application-optimized contrasts using different flip angle evolutions (SPACE), balanced steady-state free precession and turbo spin echo driven equilibrium. However, it is difficult for HR T2WI to distinguish the relationship between nerves and blood vessels when they are in close contact or there is a lack of CSF signal contrast around them. In that case, another MRI sequence is needed to assist with the diagnosis (6). Due to their advantages and disadvantages, they are frequently used together to detect NVC. Although the combination of the two sequences may make up for certain shortcomings, both display two-dimensional images, and the spatial structure of CPA cannot be displayed intuitively and dynamically. Therefore, it is necessary to identify more accurate imaging or post-processing technology to improve imaging quality.

Multimodal image fusion (MIF) may combine two or more images from the same or different modalities and reconstruct a 3D model, which allows the operator to observe anatomical details more clearly from different angles (7). Therefore, the MIF technique combined with these MRI sequences is considered to be an accurate method for the preoperative diagnosis of NVC. 3D MIF based on 3D TOF MRA combined with HR T2WI may accurately display the precise anatomical structures at the REZ and indicate the relationship between cranial nerves and blood vessels (8,9). However, there remains a lack of large-scale clinical trials to analyze its clinical application value in the preoperative diagnosis of NVC.

The present meta-analysis was designed to evaluate the value of 3D MIF based on 3D TOF MRA combined with HR T2WI in the preoperative judgment of NVC in patients with TN and HFS, and thus to evaluate its clinical application value in the preoperative evaluation of MVD.

## Materials and methods

*Manuscript preparation.* The whole study was conducted according to the PRISMA 2020 statement (10) and the manuscript was prepared and revised according to the PRISMA 2020 Checklist.

*Search strategy and selection criteria.* PubMed (<https://pubmed.ncbi.nlm.nih.gov/>), Embase (<https://www.embase.com>), Web of Science (<https://www.webofscience.com>), Scopus (<https://www.scopus.com>), China National Knowledge Infrastructure (<https://www.cnki.net>) and the Cochrane Library (<https://www.cochranelibrary.com/>) were systematically searched. The medical subject heading terms or Emtree terms

were ‘Magnetic Resonance Angiography’ and ‘Microvascular Decompression Surgery’. The search query was ‘((Microvascular Decompression Surgery) OR (Decompression Surgeries, Microvascular) OR (Decompression Surgery, Microvascular) OR (Microvascular Decompression Surgeries) OR (Surgeries, Microvascular Decompression) OR (Surgery, Microvascular Decompression) OR (Microvascular Decompression) OR (Decompression, Microvascular) OR (Decompressions, Microvascular) OR (Microvascular Decompressions)) AND ((Magnetic Resonance Angiography) OR (MRI Angiography) OR (Angiographies, MRI) OR (Angiography, MRI) OR (MRI Angiographies) OR (MRI Angiographies) OR (Angiographies, Magnetic Resonance) OR (Magnetic Resonance Angiographies) OR (Perfusion Magnetic Resonance Imaging) OR (Perfusion Weighted MRI) OR (MRI, Perfusion Weighted) OR (time-of-flight))’. Articles published from the inception of each database to September 2022 were retrieved.

After deleting duplicate publications, reasonable inclusion and exclusion criteria were developed to review the remaining studies. The inclusion criteria were as follows: i) The study used 3D MIF technology based on 3D TOF MRA combined with HR T2WI to judge NVC in patients with TN or HFS; ii) the study design was prospective or retrospective; and iii) the intraoperative findings were used as the reference standard for NVC diagnosis. The exclusion criteria were as follows: i) Reviews, case reports, editorials, correspondences, comments or meeting abstracts/meeting minutes; ii) 3D MIF technology was not used in the study, or 3D TOF MRA combined with HR T2WI was not used to fuse the multimodal image; iii) the patients in the study received only preoperative evaluation but not MVD; and iv) studies without sufficient data to construct the 2x2 contingency table.

*Data extraction.* A total of two investigators (BZ and RL) independently extracted the data, including the quality assessment of the retrieved studies. Discrepancies were resolved in a consensus meeting, or if no agreement could be reached, such as regarding the methodological quality of the included studies, they were resolved by referral to a third investigator (SG). The extracted data included the following: i) Basic research information, including the name of the first author, publication year, country of the first author, sample size and type of research design; ii) the characteristics of the participants, including the age of the patients and their diagnosis; iii) the MRI sequences used in the study; iv) the 3D fusion software used in the study; and v) the research results, including the number of true positives, false positives, false negatives, true negatives, sensitivity and specificity.

*Literature quality assessment.* The methodological quality of the included studies was assessed by two researchers on the basis of the Quality Assessment of Diagnostic Accuracy Studies (QUADAS) checklist (11). Review Manager 5.4.1 software (The Cochrane Collaboration) was used to generate a methodological quality graph and methodological quality graph summary.

*Statistical analysis.* An exact binomial rendition of the bivariate mixed-effects regression model was used to synthesize data. The data analysis was performed using the meta-analytical integration of diagnostic test accuracy studies

Table I. Basic characteristics of the included studies.

First author, year	Country	Sample size	Age, years	Diagnosis	Research type	MRI sequences	3D fusion software	True- pos	False- pos	False- neg	True- neg	Sensitivity	Specificity	(Refs.)
Shi, 2022	China	40	49.6 (24-66)	HFS	Retrospective	3D TOF MRA + 3D FIESTA	3D-slicer	38	1	0	1	1.00	0.50	(8)
Jiao, 2019	China	48	ND	TGN	Retrospective	3D TOF MRA + 3D FIESTA	3D-slicer	46	0	1	1	0.98	1.00	(12)
Yao, 2018	China	42	51.2±11.6 (22-76)	TGN/HFS	Prospective	3D TOF + 3D SPACE	3D-slicer	40	0	1	1	0.98	1.00	(9)
Dolati, 2015	USA	14	65±10	TGN	Prospective	3D TOF + 3D SPACE	iPlan Net	19	0	0	1	1.00	1.00	(15)
Dolati, 2015	USA	6	61±7	HFS										(15)
Lee, 2014	USA	190	56±14.2	TGN	Retrospective	3D TOF + bFFE	OsiriX	148	5	6	31	0.96	0.86	(13)
Miller, 2008	USA	18	52.9 (26-80)	TGN	Prospective	3D TOF + bFFE + 3D Gd-enhanced SPGR	OsiriX	15	0	1	2	0.94	1.00	(14)
Granata, 2013	Italy	32	42±7 (23-68)	TGN/ HFS	Prospective	3D TOF + 3D CISS	Leonardo	21	0	0	11	1.00	1.00	(16)

Values are expressed as the median (range) and/or mean ± standard deviation. ND, no data; TOF MRA, time-of-flight magnetic resonance angiography; FIESTA, fast imaging employing steady-state acquisition; SPACE, sampling perfection with application-optimized contrasts using different flip angle evolutions; bFFE, balanced fast field echo; SPGR, spoiled gradient recalled; CISS, constructive interference steady state; TN, trigeminal neuralgia; HFS, hemifacial spasm; Pos, positive; Neg, negative.

(MIDAS) module of Stata 16.0 software (StataCorp LP). The pooled sensitivity, specificity, positive likelihood ratio (PLR), negative likelihood ratio (NLR), diagnostic odds ratio (DOR), area under the receiver operating characteristic curve (AUROC) and 95% CIs were calculated. The  $I^2$  and Q-test were used to assess heterogeneity. The publication bias of the included literature was examined by Deeks' test using Stata 16.0. The clinical application value of 3D MIF based on 3D TOF MRA combined with HR T2WI for the diagnosis of NVC was evaluated by Fagan nomogram and likelihood ratio (LR) scatter plot. Graphs were produced using the MIDAS module for Stata 16.0 and Review Manager 5.4.1 software.

## Results

**Included articles.** In the search, 702 articles were identified, with 435 articles remaining after discarding duplicate records. A full-text analysis was performed on the 56 articles that remained following screening by titles and abstracts, of which 6 articles did not have complete data and 43 articles were not related to 3D MIF or 3D TOF MRA combined with HR T2WI, and were therefore excluded. Finally, 7 articles were included in the present analysis (Fig. 1).

**Basic characteristics of the included studies.** The basic characteristics of the studies included in the present meta-analysis are presented in Table I. A total of 390 patients were included in the seven studies. Among them, three studies (12-14) focused on TN, one (8) on HFS and three (9,15,16) on both. A total of two (8,12) of the seven studies performed 3D TOF MRA combined with the 3D FIESTA sequence, two (9,15) performed 3D TOF MRA combined with the 3D SPACE sequence, one (13) performed 3D TOF MRA combined with bFFE sequence, one (14) performed 3D TOF MRA combined with bFFE and 3D Gd-enhanced spoiled gradient recalled sequence, and one (16) performed 3D TOF MRA combined with the 3D CISS sequence. A total of three (8,9,12) of the seven studies used 3D-slicer software (17) for 3D MIF, two (13,14) used OsiriX 2.5.1 software (Pixmeo SARL), and the remaining two used iPlan Net (Brainlab AG) (15) software and Leonardo™ (Siemens AG) software (16), respectively. A total of four studies (9,14-16) were performed as prospective studies and the remaining three as retrospective studies. According to the methodological quality graph (Fig. 2A) and the methodological quality summary (Fig. 2B), the quality of the literature included in the present study was acceptable.

### Meta-analysis results

**Heterogeneity of the meta-analysis.** The  $I^2$  and Q-test were used to assess the heterogeneity of the studies. The results indicated that the studies in the present meta-analysis had no substantial heterogeneity ( $I^2=0$ ;  $Q=0.000$ ;  $P=0.50$ ). The same result was observed from the Galbraith plot (Fig. 3A).

**Summary effect size.** Bivariate analysis yielded that the pooled sensitivity and specificity of 3D MIF based on 3D TOF MRA combined with HR T2WI for detecting NVC were 0.97 (95% CI, 0.95-0.99) and 0.89 (95% CI, 0.77-0.95), respectively (Fig. 4A). The pooled PLR was 8.8 (95% CI, 4.1-18.6), the pooled NLR was 0.03 (95% CI, 0.02-0.06; Fig. 4B) and the

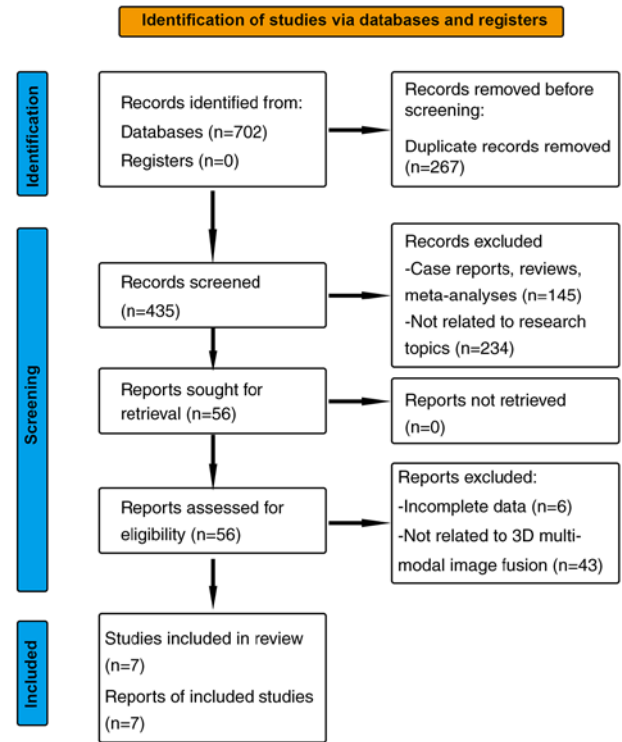


Figure 1. Flow chart of the literature search and results of the present meta-analysis.

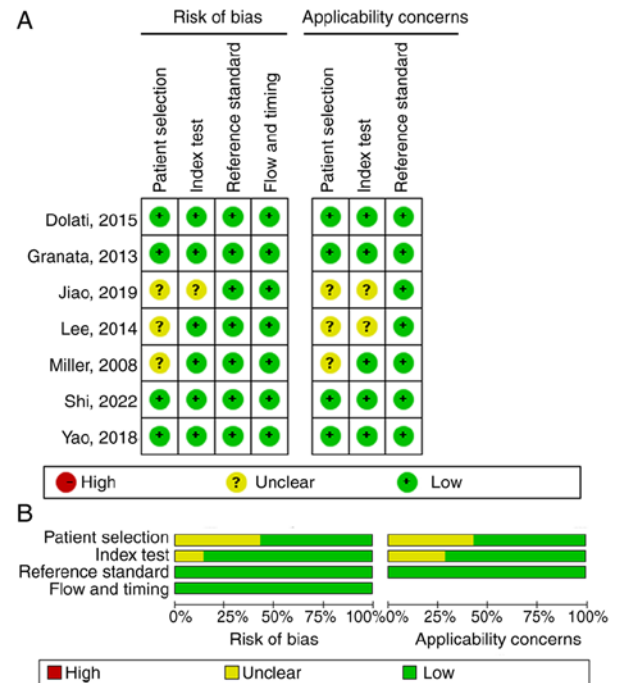


Figure 2. Methodological quality of the included studies was assessed using the Quality Assessment of Diagnostic Accuracy Studies checklist. (A) Methodological quality graph. (B) Methodological quality summary.

pooled DOR was 291 (95% CI, 99-853; Fig. 4C). The AUROC was 0.98 (95% CI, 0.97-0.99; Fig. 4D).

**Publication bias.** The Deeks' funnel plot asymmetry test was used to evaluate the publication bias of the studies in the

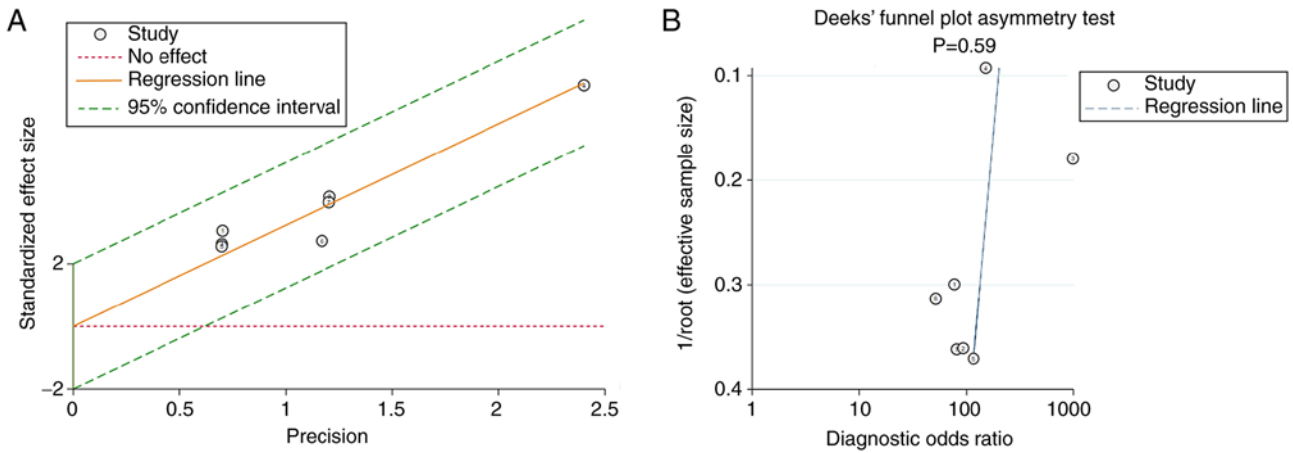


Figure 3. Heterogeneity and publication bias of the present meta-analysis. (A) Galbraith plot. (B) Deeks' funnel plot.

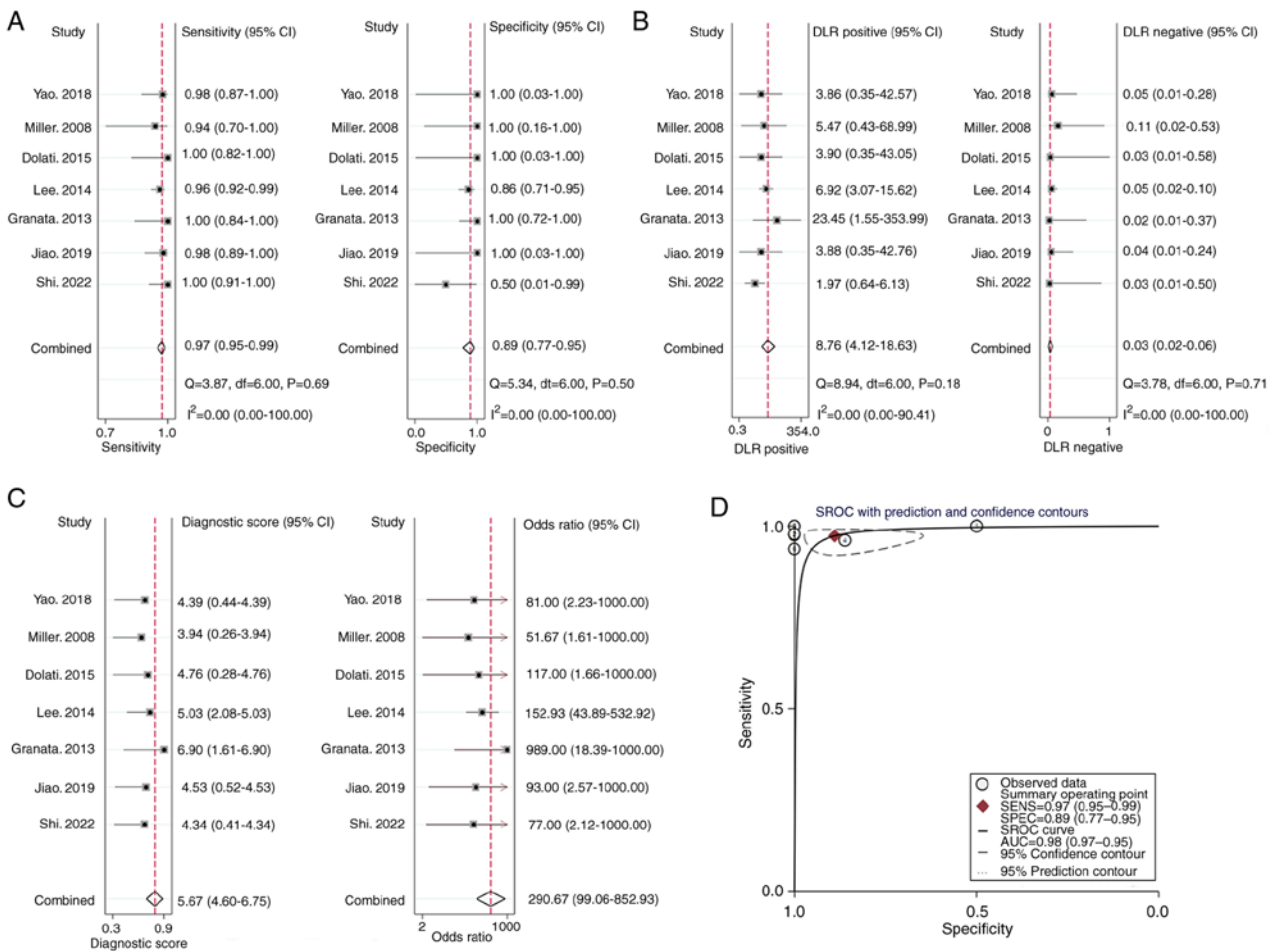


Figure 4. Summary effect size of the present meta-analysis. (A) Pooled sensitivity and specificity. (B) Pooled positive likelihood ratio and pooled negative likelihood ratio. (C) Pooled diagnostic odds ratio. (D) SROC curve. DLR, diagnostic likelihood ratio; SROC, summary receiver operating characteristic; SENS, sensitivity; SPEC, specificity; AUC, area under the curve.

current meta-analysis, with P=0.59 indicating no significant publication bias in the included studies (Fig. 3B).

**Sensitivity analysis.** Sensitivity analysis was carried out by deleting each included study one by one and calculating the respective summary effect size. The pooled sensitivity and AUROC were used as evaluation indicators. The results

suggested that excluding any study did not significantly change the pooled sensitivity and AUROC (Table II), indicating that the results of the present meta-analysis were robust and reliable.

**Evaluation of clinical application value.** The LR scatter plot based on summary PLR and NLR was in the lower left quadrant (Fig. 5A). According to the data of the present meta-analysis,

Table II. Sensitivity analysis.

First author of excluded study, year	Pooled sensitivity (95% CI)	Pooled AUROC (95% CI)	(Refs.)
Shi, 2022	0.97 (0.93-0.99)	0.98 (0.97-0.99)	(8)
Jiao, 2019	0.97 (0.95-0.99)	0.98 (0.97-0.99)	(12)
Yao, 2018	0.97 (0.95-0.99)	0.98 (0.97-0.99)	(9)
Dolati, 2015	0.97 (0.95-0.99)	0.98 (0.97-0.99)	(15)
Lee, 2014	0.98 (0.95-1.00)	0.99 (0.98-1.00)	(13)
Miller, 2008	0.97 (0.95-0.99)	0.98 (0.97-0.99)	(14)
Granata, 2013	0.97 (0.95-0.99)	0.98 (0.96-0.99)	(16)

AUROC, area under the receiver operating characteristic curve.

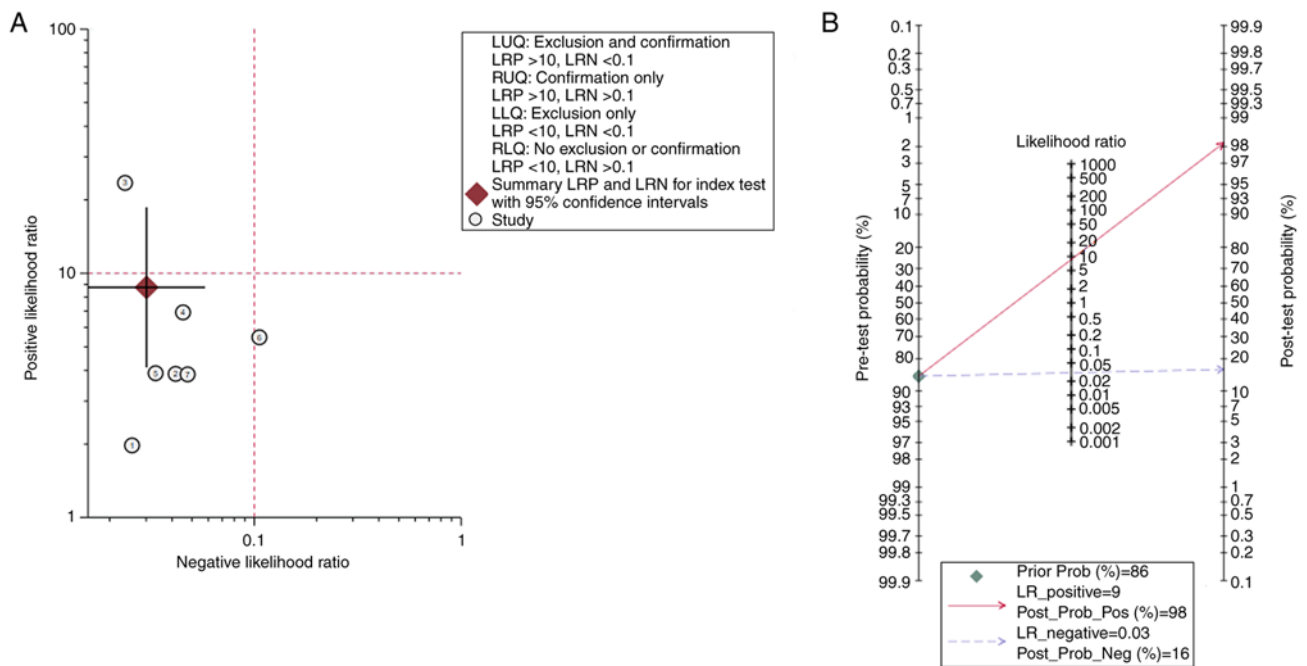


Figure 5. Assessment of the clinical application value of 3D multimodal image fusion based on time-of-flight magnetic resonance angiography combined with high-resolution T2-weighted imaging. (A) Likelihood ratio scatter plot. (B) Fagan nomogram showing the post-test probability. LUQ, left upper quadrant; LRP, likelihood ratio positive; LRN, likelihood ratio negative; RUQ, right upper quadrant; LLQ, left lower quadrant; RLQ, right lower quadrant; LR, likelihood ratio; Prob, probability; Pos, positive; Neg, negative.

the incidence rate of NVC in patients with TN and HFS was estimated to be 86.15%, which was consistent with the reported results (18). Therefore, with a pretest probability of 0.86, the Fagan nomogram indicated that the positive post-test probability was 98% and the negative post-test probability 16% (Fig. 5B).

## Discussion

In the present meta-analysis, the sensitivity, specificity, PLR, NLR, DOR and AUROC of 3D MIF based on 3D TOF MRA combined with HR T2WI for detecting NVC were examined. The results demonstrated a high diagnostic ability of this technology with high sensitivity and specificity. As mentioned above, 3D TOF MRA is a widely used MRI sequence for detecting NVC, which is frequently used as a

standard MRI-based method to compare with other methods. In a previous meta-analysis, the authors reported that 3D TOF MRA exhibited a sensitivity of 0.95 (95% CI, 0.93-0.96) and specificity of 0.77 (95% CI, 0.66-0.86) in correctly identifying NVC in patients with TN (19). According to the present results, when using 3D MIF technology, the sensitivity and specificity in diagnosing NVC was able to be improved. In a previous report, the DOR and AUROC of 3D TOF MRA in diagnosing NVC were 52.92 (95% CI, 26.39-106.11) and 0.97 (95% CI, 0.95-0.99), respectively (19). Compared with 3D TOF MRA, the DOR of 3D MIF technology based on 3D TOF MRA combined with HR T2WI reached 291 (95% CI, 99-853) and the AUROC was 0.98 (95% CI, 0.97-0.99). These results suggested that compared with 3D TOF MRA, 3D MIF technology based on 3D TOF MRA combined with HR T2WI appears to have more advantages in

diagnosing NVC in terms of diagnostic accuracy. In addition, whether 3D MIF is able to actually improve the effectiveness of 3D TOF MRA combined with HR T2 in the diagnosis of NVC is also of great concern. In another meta-analysis, the sensitivity and specificity of 3D TOF MRA combined with HR T2WI in diagnosing NVC were 0.96 (95% CI, 0.92-0.98) and 0.92 (95% CI, 0.74-0.98), respectively, and the DOR and AUROC were 283 (95% CI, 50-1,620) and 0.98 (95% CI 0.97-0.99), respectively (20). Compared with the results of the present study, the sensitivity and DOR of the diagnosis of NVC appear to be improved after the combination of 3D MIF technology. However, it is not accurate to evaluate the diagnostic effectiveness of different methods by directly comparing the values of different meta-analysis results. In a network meta-analysis, different NVC diagnostic methods were evaluated by constructing statistical models, and the results indicated that 3D MIF based on 3D TOF MRA combined with HR T2WI did have a higher superiority index in diagnosing NVC compared with the simple combination of the aforementioned MRI sequences without 3D MIF (21). These results suggested that 3D MIF technology may indeed improve the efficiency of NVC diagnosis.

To date, to the best of our knowledge, no meta-analysis has been published on HR T2WI as another type of MRI sequence commonly used in the detection of NVC. Therefore, there are no indicators that may accurately reflect the ability of HR T2WI to detect NVC, such as the pooled sensitivity, specificity, PLR, NLR, DOR and AUROC. According to existing clinical studies, the range of sensitivity and specificity of HR T2 WI in the detection of NVC are 86.17-100 and 71.47-100%, respectively (22-25). The results of different studies vary widely, which may be due to the use of different HR T2WI techniques and study designs. The value of HR T2WI in detecting NVC requires to be evaluated by further meta-analyses or large-scale clinical studies. Current data cannot be used to directly compare the ability of HR T2WI and 3D MIF based on 3D TOF MRA combined with HR T2WI to detect NVC.

Furthermore, the post-test probabilities are also associated with the clinical diagnostic ability of the diagnostic test (26). In the present study, the post-test probability for a positive test result was 98%, indicating the high clinical application value of 3D MIF based on 3D TOF MRA combined with HR T2WI in diagnosing NVC. The LR scatter plot is a qualitative effect size rating approach for diagnostic test accuracy, which divides the effect rating of diagnostic tests by quadrant (27). The LR scatter plot based on summary PLR and NLR was in the lower left quadrant. This meant that 3D MIF based on 3D TOF MRA combined with HR T2WI has the ability to exclude the diagnosis of NVC and that the diagnostic accuracy of this test has a 'moderate' effect rating. In combination, the above two results suggested that 3D MIF based on 3D TOF MRA combined with HR T2WI had a good clinical application value in diagnosing NVC.

For 3D MIF, the selection of MR sequences for fusion also affects the final diagnostic effect. Since the combination of 3D TOF MRA and HR T2WI has several advantages in detecting NVC (28,29), it may add to the advantages of 3D MIF technology. In fact, this is also the most commonly used combination of MRI sequences in 3D MIF clinical studies to detect NVC (8,9,12-16). There are currently few studies on the

use of other MRI sequence combinations for 3D MIF in the detection of NVC (30). However, with the development of MR technology, other more suitable MRI sequence combinations may appear.

The present meta-analysis had certain limitations: i) NVC may also cause glossopharyngeal neuralgia (GN), but due to the lack of relevant clinical research data, patients with GN were not included in the current meta-analysis; ii) due to the limited number of cases, subgroup analyses were not performed for different diseases, T2 sequences or 3D fusion software; iii) of the seven included studies, three were retrospective studies, which have more potential sources of bias and confounding than prospective studies.

In conclusion, the present results suggested that 3D MIF based on 3D TOF MRA combined with HR T2WI has excellent sensitivity and specificity for detecting NVC in patients with TN or HFS. This method should serve a key role in the preoperative evaluation of MVD.

### Acknowledgements

Not applicable.

### Funding

The present study was supported by a grant from the Key Research and Development Plan of Shaanxi Province, China (grant no. 2021SF-298).

### Availability of data and materials

The datasets used and/or analyzed during the current study are available from the corresponding author on reasonable request.

### Authors' contributions

CL was responsible for writing the main manuscript and data analysis. CL and LY contributed to the study design. BZ, SG and RL contributed to the literature search, data extraction and quality assessment. CL and SG confirm the authenticity of all the raw data. All authors have read and approved the final manuscript.

### Ethics approval and consent to participate

Not applicable.

### Patient consent for publication

Not applicable.

### Competing interests

The authors declare that they have no competing interests.

### References

1. Broggi M, Acerbi F, Ferroli P, Tringali G, Schiariti M and Broggi G: Microvascular decompression for neurovascular conflicts in the cerebello-pontine angle: which role for endoscopy? *Acta Neurochir (Wien)* 155: 1709-1716, 2013.



2. Cui Z and Ling Z: Advances in microvascular decompression for hemifacial spasm. *J Otol* 10: 1-6, 2015.
3. Sade B and Lee JH: Microvascular decompression for trigeminal neuralgia. *Neurosurg Clin N Am* 25: 743-749, 2014.
4. Montano N, Conforti G, Di Bonaventura R, Meglio M, Fernandez E and Papacci F: Advances in diagnosis and treatment of trigeminal neuralgia. *Ther Clin Risk Manag* 11: 289-299, 2015.
5. Chen SR: Neurological Imaging for Hemifacial Spasm. *Int Ophthalmol Clin* 58: 97-109, 2018.
6. Donahue JH, Ornan DA and Mukherjee S: Imaging of Vascular Compression Syndromes. *Radiol Clin North Am* 55: 123-138, 2017.
7. Huang B, Yang F, Yin M, Mo X and Zhong C: A Review of multimodal medical image fusion techniques. *Comput Math Methods Med* 2020: 8279342, 2020.
8. Shi H, Li Y, Wang Y, Guo W, Zhang K, Du Y, Shi H and Qian T: The preoperative evaluation value of 3D-slicer program before microsurgical vascular decompression in patients with hemifacial spasm. *Clin Neurol Neurosurg* 217: 107241, 2022.
9. Yao S, Zhang J, Zhao Y, Hou Y, Xu X, Zhang Z, Kikinis R and Chen X: Multimodal image-based virtual reality presurgical simulation and evaluation for trigeminal neuralgia and hemifacial spasm. *World Neurosurg* 113: e499-e507, 2018.
10. Page MJ, McKenzie JE, Bossuyt PM, Boutron I, Hoffmann TC, Mulrow CD, Shamseer L, Tetzlaff JM, Akl EA, Brennan SE, *et al*: The PRISMA 2020 statement: An updated guideline for reporting systematic reviews. *BMJ* 372: n71, 2021
11. Whiting PF, Rutjes AW, Westwood ME, Mallett S, Deeks JJ, Reitsma JB, Leeflang MM, Sterne JA, Bossuyt PM and QUADAS-2 Group: QUADAS-2: A revised tool for the quality assessment of diagnostic accuracy studies. *Ann Intern Med* 155: 529-536, 2011.
12. Jiao Y, Duan F, Yan Z, Meng Q and Feng Y: The value of 3D-TOF-MRA and 3D-FIESTA fusion three-dimensional images in judgment of offending vessel in primary trigeminal neuralgia. *Chin J Neurosurg* 35: 928-932, 2019.
13. Lee A, McCartney S, Burbidge C, Raslan AM and Burchiel KJ: Trigeminal neuralgia occurs and recurs in the absence of neurovascular compression Clinical article. *J Neurosurg* 120: 1048-1054, 2014.
14. Miller J, Acar F, Hamilton B and Burchiel K: Preoperative visualization of neurovascular anatomy in trigeminal neuralgia. *J Neurosurg* 108: 477-482, 2008.
15. Dolati P, Golby A, Eichberg D, Abolfotoh M, Dunn IF, Mukundan S, Hulou MM and Al-Mefty O: Pre-operative image-based segmentation of the cranial nerves and blood vessels in microvascular decompression: Can we prevent unnecessary explorations? *Clin Neurol Neurosurg* 139: 159-165, 2015.
16. Granata F, Vinci SL, Longo M, Bernava G, Caffo M, Cutugno M, Morabito R, Salamone I, Tomasello F and Alafaci C: Advanced virtual magnetic resonance imaging (MRI) techniques in neurovascular conflict: Bidimensional image fusion and virtual cisternography. *Radiol Med* 118: 1045-1054, 2013.
17. Fedorov A, Beichel R, Kalpathy-Cramer J, Finet J, Fillion-Robin JC, Pujol S, Bauer C, Jennings D, Fennessy F, Sonka M, *et al*: 3D Slicer as an image computing platform for the quantitative imaging network. *Magn Reson Imaging* 30: 1323-1341, 2012.
18. Bašić Kes V and Zadro Matovina L: Accommodation to diagnosis of trigeminal neuralgia. *Acta Clin Croat* 56: 157-161, 2017.
19. Cai J, Xin ZX, Zhang YQ, Sun J, Lu JL and Xie F: Diagnostic value of 3D time-of-flight MRA in trigeminal neuralgia. *J Clin Neurosci* 22: 1343-1348, 2015.
20. Liang C, Yang L, Zhang BB, Guo SW and Li RC: Three-dimensional time-of-flight magnetic resonance angiography combined with high resolution T2-weighted imaging in preoperative evaluation of microvascular decompression. *World J Clin Cases* 10: 12594-12604, 2022.
21. Liang C, Yang L, Reichardt W, Zhang B and Li R: Different MRI-based methods for the diagnosis of neurovascular compression in trigeminal neuralgia or hemifacial spasm: A network meta-analysis. *J Clin Neurosci* 108: 19-24, 2022.
22. Xia H, Kong M, Lu H, Luo S, Xu D and Zhang J: Value of MR 3D FLASH-WE combined with 3D SPACE sequences applied in cranial nerve diseases. *Chin Comput Med Imaging* 21: 505-509, 2015 (In Chinese).
23. Jia JM, Guo H, Huo WJ, Hu SW, He F, Sun XD and Lin GJ: Preoperative evaluation of patients with hemifacial spasm by three-dimensional time-of-flight (3D-TOF) and three-dimensional constructive interference in steady state (3D-CISS) sequence. *Clin Neuroradiol* 26: 431-438, 2016.
24. Ruiz-Juretschke F, Guzmán-de-Villoria JG, García-Leal R and Sañudo JR: Predictive value of magnetic resonance for identifying neurovascular compressions in trigeminal neuralgia. *Neurologia* 34: 510-519, 2019 (In English, Spanish).
25. Yang D, Shen J, Xia X, Lin Y, Yang T, Lin H, Jin Y, Zhou K and Li Y: Preoperative evaluation of neurovascular relationship in trigeminal neuralgia by three-dimensional fast low angle shot (3D-FLASH) and three-dimensional constructive interference in steady-state (3D-CISS) MRI sequence. *Br J Radiol* 91: 20170557, 2018.
26. Gogtay NJ: Statistical evaluation of diagnostic tests-part 2 (pre-test and post-test probability and odds, likelihood ratios, receiver operating characteristic curve, Youden's index and diagnostic test biases). *J Assoc Physicians India* 65: 86-91, 2017.
27. Rubinstein ML, Kraft CS and Parrott JS: Determining qualitative effect size ratings using a likelihood ratio scatter matrix in diagnostic test accuracy systematic reviews. *Diagnosis* 5: 205-214, 2018.
28. Singhal S and Danks RA: Radiologic and neurosurgical diagnosis of arterial neurovascular conflict on magnetic resonance imaging for trigeminal neuralgia in routine clinical practice. *World Neurosurg* 157: e166-e172, 2022.
29. Wei Sheng C, Yu R, Meng Q and Qu C: Efficacy of microvascular decompression in patients with trigeminal neuralgia with negative neurovascular relationship shown by magnetic resonance tomography. *Clin Neurol Neurosurg* 197: 106063, 2020.
30. Ogiwara M and Shimizu T: Surface rendered three-dimensional MR imaging for the evaluation of trigeminal neuralgia and hemifacial spasm. *J Clin Neurosci* 11: 840-844, 2004.



This work is licensed under a Creative Commons Attribution-NonCommercial-NoDerivatives 4.0 International (CC BY-NC-ND 4.0) License.